Journal of Nuclear Materials 405 (2010) 261–265

Contents lists available at ScienceDirect

Journal of Nuclear Materials

journal homepage: www.elsevier.com/locate/jnucmat

Anomaly in dependence of radiation-induced vacancy accumulation on grain size

Yi Yang [a], Hanchen Huang [a,b,*], Steven J. Zinkle [c]

[a] Department of Mechanical, Aerospace and Nuclear Engineering, Rensselaer Polytechnic Institute, Troy, NY 12180, USA
[b] Department of Mechanical Engineering, University of Connecticut, Storrs, CT 06269, USA
[c] Materials Science and Technology Division, Oak Ridge National Laboratory, Oak Ridge, TN 37831, USA

ARTICLE INFO

Article history:
Received 8 February 2010
Accepted 14 August 2010

ABSTRACT

According to conventional steady-state rate theory predictions of displacement damage evolution in irradiated materials, the accumulation of vacancies decreases as grain size decreases. Using atomistic simulations, the authors report a transient anomaly in the dependence of radiation produced vacancy accumulation on grain size. Contrary to the conventional wisdom, the accumulation of vacancies can be higher in smaller grains than in larger grains during a transient stage. The anomaly is a result of competition between two atomic-level processes: grain boundary absorption and bulk recombination of point defects, each of which has characteristic length and time scales. Copper is used as the prototype of face-centered-cubic material and Frenkel pair production mimicking electron radiation is the source of non-cascade defect introduction, both choices aiming at clarity for identifying physical mechanisms.

1. Introduction

The radiation of polycrystalline metals by energetic beams including electrons, neutrons, and ions produces both vacancies and interstitials along with their clusters under cascade conditions, and gas impurity atoms under transmutation conditions [1–3]. Electron radiation, which produces individual vacancies and interstitials, is a convenient experimental tool for studying fundamental point defect processes, versus more complex processes involving displacement cascade production and transmutations associated with energetic neutron radiation. Electron radiation experiments also provide validation to the conventional rate theories, which in turn form the basis of more advanced models such as the production bias model [4] for cascade production conditions. This path from simple to complex processes is particularly conducive in revealing generic mechanisms of radiation damage.

For the simple case of electron radiation, it is known that defect accumulation decreases as grain size decreases for steady-state conditions [5]. This monotonic dependence is the result of defects diffusing to grain boundaries (GBs) where they are annihilated, and it is true provided that production and annihilation of defects have reached a steady state. During the transient stage before steady-state conditions are achieved, the intricate balance of defect populations may result in different dependencies of defect accumulation on grain size. The time to reach steady state depends on the slowest process, such as vacancy diffusion in metals and defect clustering. Since the transient time can be long, what happens during this stage can be interesting from both scientific and technological perspectives. Based on atomistic simulations, this paper reports a transient anomaly (or crossover) in the dependence of defect accumulation on grain size that is the result of kinetic differences in two competing atomic processes – GB absorption and bulk recombination.

2. Simulation methods

The atomistic simulations are based on the ADEPT numerical package [6], which is an extension of conventional lattice kinetic Monte Carlo methods. The extension enables the representation of multiple lattices and thereby polycrystalline materials. In order to represent multiple lattices, we have gone through four stages of method development. In the first stage [6], we simply assign an index to each lattice site to label a crystalline orientation. In the second stage, we map two lattices onto one lattice [7]. In the third stage, we map multiple lattices onto one lattice, in reduced two-dimensional space [8]. Finally, in the fourth stage, we map multiple lattices onto one lattice, in three-dimensional space but for simple cubic (SC) lattice only [9]. Based on the fourth stage implementation, we extend the development to face-centered-cubic (FCC) lattices in the current version of ADEPT.

An FCC lattice consists of four SC sub-lattices. Therefore, mapping of an FCC lattice becomes the mapping of four SC lattices. Taking the first SC sub-lattice as reference, the displacements of the four SC sub-lattices are [0 0 0], [1 1 0], [0 1 1], and [1 0 1]; the unit is half a lattice constant. Denoting these as position vectors of the four sub-lattices u_ε (where ε goes from 1 to 4), we can determine the relative positions of any two sub-lattices as $u_{\varepsilon\phi} = u_\varepsilon - u_\phi$. The

* Corresponding author at: Department of Mechanical Engineering, University of Connecticut, Storrs, CT 06269, USA. Tel.: +1 860 486 9037; fax: +1 860 486 5088.
E-mail address: hanchen@uconn.edu (H. Huang).

0022-3115/$ - see front matter © 2010 Elsevier B.V. All rights reserved.
doi:10.1016/j.jnucmat.2010.08.014

$u_{\varepsilon\phi}$ is always in the form of [a b 0], [a 0 b], or [0 a b], with a and b being 1 or −1. On each sub-lattice (say lattice ε), a lattice site is labeled by three indices (i, j, k), and it has 12 nearest neighbors; four from each of the other three sub-lattices. If $u_{\varepsilon\phi}$ is [0 a b], the four nearest neighbors from sub-lattice ϕ have indices (i, j, k), $(i, j + a, k)$, $(i, j, k + b)$, and $(i, j + a, k + b)$; as shown in Fig. 1. Based on this mapping process for FCC lattice, the error in representing a lattice site's position is always within two lattice periods, and it peaks at half a lattice period, as shown in Fig. 2.

Within the framework of updated ADEPT, a vacancy is an empty site in an FCC (copper in this case) lattice. Although an interstitial atom has various configurations, we place it at a site of another lattice that is identical to the copper crystal lattice. To simulate electron radiation, we introduce a pair of vacancy and interstitial defects at a production rate P (selected to be 10^{-5} displacement per atom per second (dpa/s) for all simulations in this paper). The Frenkel pair has an initial separation distance, with equal probability, between 3 and 8 lattice constants; the vacancy-interstitial recombination distance is taken to be two lattice constants, and vacancy–vacancy interaction distance is one lattice constant based on analysis of electron radiation experiments [10]. Copper is the prototype FCC material in this study, and its lattice constant is 0.361 nm at room temperature [11]. Focusing on defects, we parameterize atomic potential energy to represent formation energies of single vacancy and its clusters, and choose the potential energy E_i of an atom to be −2.11, −2.29, −2.30, −2.70, −2.85, −3.02, −3.16, −3.32, −3.43, and −3.54 eV when its coordination i goes from 3 to 12. The formation energies of small vacancy clusters given by this potential are listed in Table 1, in comparison to molecular dynamics (MD) results. In addition to potential energies, diffusion energy barriers and prefactors are also critical inputs to ADEPT. In this study, single vacancies and interstitials are the diffusing entities in bulk; no interstitial clusters form while few vacancy clusters do in our simulations. All vacancy clusters are assumed to be immobile. According to our MD simulations, the diffusion jump frequency of single vacancies is $\nu_v = 4.7 \times 10^{12} \times e^{-0.67/kT}\ s^{-1}$ and that of interstitial atoms is $\nu_i = 1.4 \times 10^{12} \times e^{-0.09/kT}\ s^{-1}$, consistent with literature data [11]; kT is the Boltzmann factor in eV.

In polycrystalline ADEPT simulations, representation of GB energetics is crucial. We use vacancies to represent GB formation volume. According to experimental data [12], the formation volume of Σ9 [0 1 1](1 2 2) GB of copper is 0.1241 nm; note, the formation volume units are volume per unit area. Atomistic simulations show that the formation volume of Σ9 [0 1 1](1 2 2) GB of copper is about 75% that of random GBs. Therefore, we estimate that the formation volume of random GBs is 0.16 nm; all GBs are random in this study. For each atom at GB, it may have n neighbors from neighboring grains. The corresponding energy of this atom is increased by $n\Delta E$, relative to its counterpart in grain interior. We choose ΔE to be 0.125 eV to reproduce the GB formation volume under thermodynamic equilibrium at room temperature. The GB vacancies are diffusing agents of GB diffusion, and change of grain orientations of GB atoms represents GB migration. In this study, all grains have the same shape and size, and all GBs are random. As a result, details of GB diffusion and migration are not critical, and will be left out.

The polycrystalline simulation cell consists of ⟨1 1 0⟩ columnar grains with hexagonal cross-sections, as shown in Fig. 3. Following Yamakov et al. [13], the four grain orientations have relative rotation angles of 0°, 30°, 60°, 90° respectively; so all GBs are random. The grain diameter L ranges from 10 nm to 50 nm, and the z dimension (thickness) is 7.5 nm; numerical tests show that the calculated single vacancy concentration is constant within 2% when

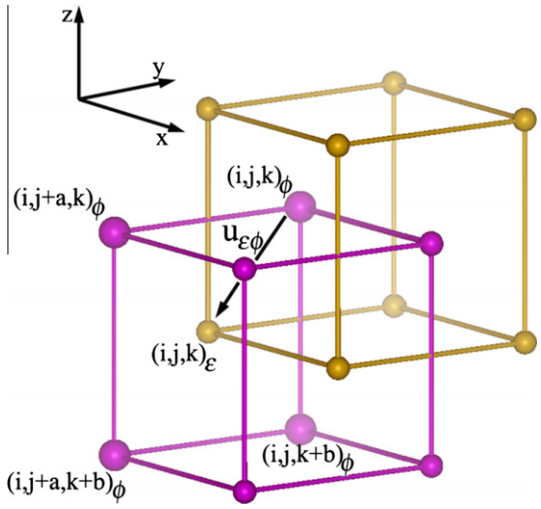

Fig. 1. Four neighbors from lattice ϕ for site $(i, j, k)_\varepsilon$, with $u_{\varepsilon\phi}$ = [0 a b] = [0 $\bar{1}$ $\bar{1}$].

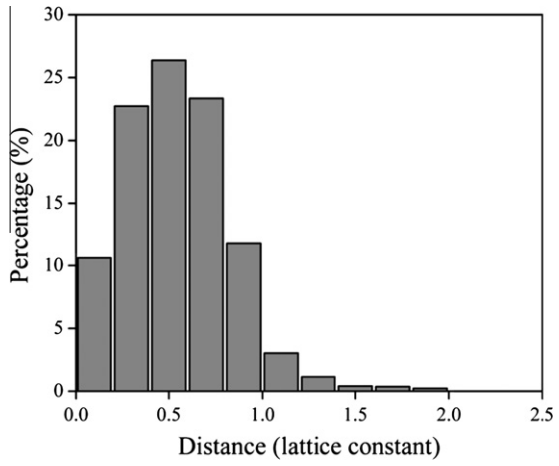

Fig. 2. Distribution of lattice sites as a function of separation between a mapped site and its physical site.

Table 1
Formation energies of small vacancy clusters.

	E_f^v	E_f^{2v}	$E_f^{3v\,a}$	$E_f^{4v\,b}$
MD	1.27	2.40	3.38	4.22
ADEPT	1.28	2.41	3.39	4.06

[a] In the shape of triangle on {1 1 1}.
[b] In the shape of tetrahedron.

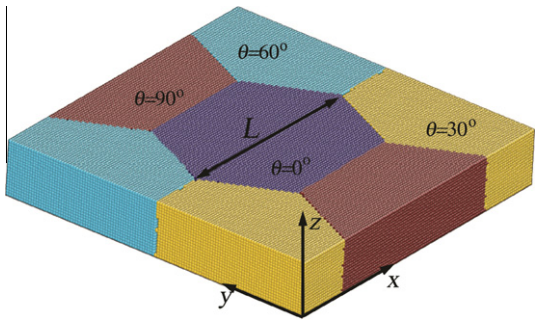

Fig. 3. Schematic of simulation cell, with grain size L and rotation angle θ labeled.

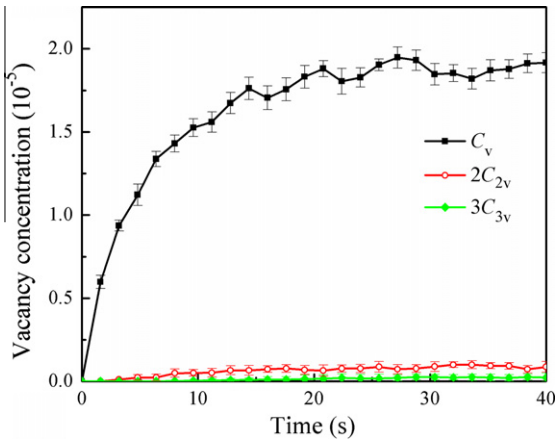

Fig. 4. Vacancy concentrations as a function of radiation time for $T = 0.25T_m$.

the z dimension is increased to 15 nm. Periodical boundary conditions are applied in all three directions.

3. Simulation results

Due to the high mobility of interstitial atoms, the accumulated defects are single vacancies and vacancy clusters only. Fig. 4 shows the monovacancy concentration C_v, defined as the ratio of number of single vacancies and the total number of grain interior lattice sites, as a function of time; here, $L = 40$ nm, $P = 10^{-5}$ dpa/s, $T = 0.25T_m$ (T_m is the melting temperature, 1357 K). The concentration is the average of 20 independent simulations, and the error bar of each data point is twice the standard deviation among the 20 simulations. Also included in the figure are the concentrations of vacancy clusters C_{2v} and C_{3v}. The concentration of divacancy clusters is already substantially smaller than that of monovacancy, and the concentration of trivacancy (or larger clusters) is negligibly small. Most vacancies are in the form of monovacancies for simulation times up to 35 s.

The total vacancy concentration, i.e. sum of C_v, $2C_{2v}$, $3C_{3v}$, and so on, depends on grain size also. In Fig. 5a, we show the total vacancy concentration within 8 s for three different grain sizes. At short times, say 0.8 s, the total vacancy concentration in smaller grains is monotonically higher than in larger grains; this is the opposite dependence on grain size compared to classical steady-state point defect radiation conditions [5]. As radiation continues, for example to 6.8 s, a non-monotonic dependence on grain size (crossover) results. As radiation continues even further, for example to 30 s, Fig. 5b shows a monotonic increase with increasing grain size, similar to the classical behavior reported in [5].

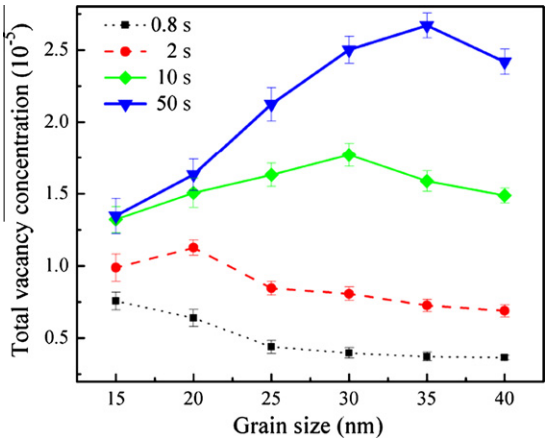

Fig. 6. Snapshots of total vacancy concentration as a function of grain size at $T = 0.25T_m$; the error bars are defined in the same way as in Fig. 4.

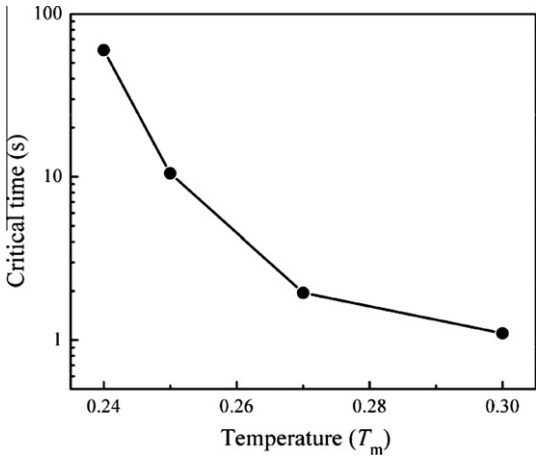

Fig. 7. Critical time for the crossover transition in vacancy concentration for 25 versus 40 nm grain sizes as a function of radiation temperature.

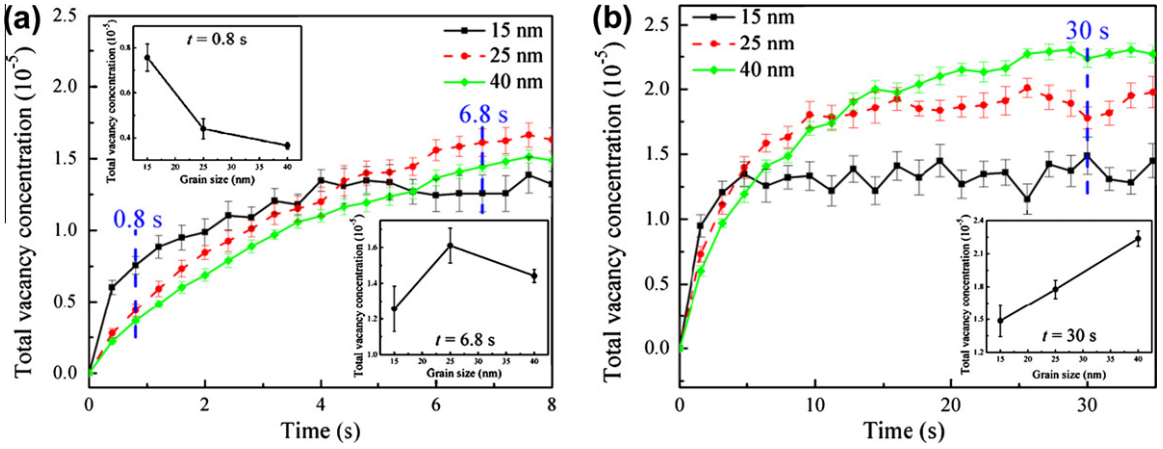

Fig. 5. Total vacancy concentration at $T = 0.25T_m$ as a function of time for three different grain sizes: (a) within 8 s, and (b) within 35 s; the error bars are defined in the same way as in Fig. 4.

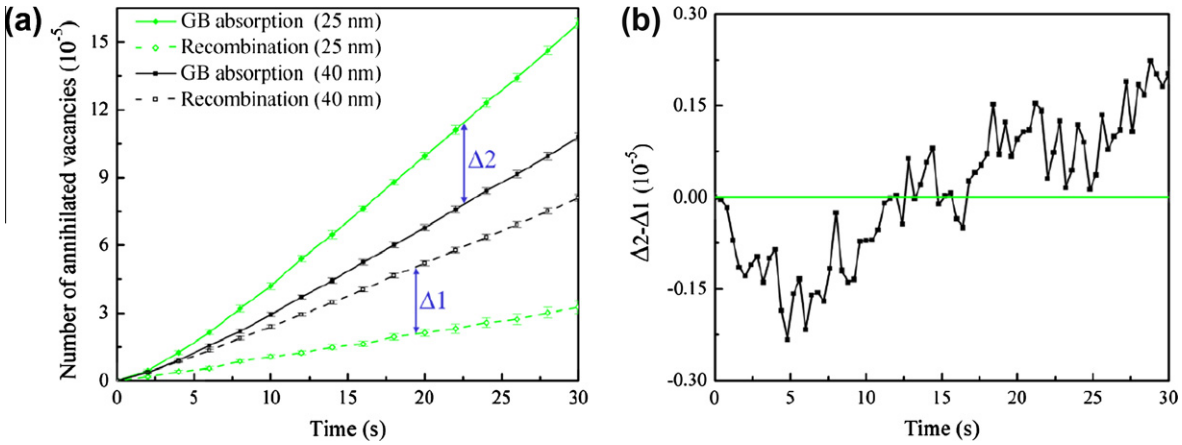

Fig. 8. (a) Number of annihilated vacancies at $T = 0.25T_m$ (normalized by the number of grain interior lattice sites) as a function of time for grain sizes of 25 and 40 nm, and (b) comparison of the relative importance of GB absorption versus bulk recombination for the two grain sizes, $\Delta 2 - \Delta 1$.

As depicted in the inset plots in Fig. 5, the dependence of total vacancy concentration on grain size goes through three stages in time: monotonic decrease, crossover, and monotonic increase; the last stage being consistent with the dependence at steady state. If we take steady state dependence as the norm, the anomaly for smaller grains will transition into the norm faster. For example, the dependence for grain sizes of 15 nm and 25 nm transitions to the norm at about 4 s, while that for grain sizes of 25 nm and 40 nm occurs at about 10 s. Fig. 6 shows that as time goes on, the grain size where the crossover transition occurs steadily increases. While the crossover transition at 50 s occurs around grain size of 35 nm, similar transition at much later time (hours or days) will occur around much larger grain sizes. In addition, since accumulated defects will interact with dislocations in highly non-linear fashion, the anomaly at early time of 50 s or so will have impacts to long-time evolution of defects in nuclear materials.

To clearly reveal the competition of kinetic effects, we consider two grains of 25 nm and 40 nm under various radiation temperatures; temperature affects kinetic rates. At an early stage, total vacancy concentration is higher for grains of 25 nm in size than for 40 nm. After a critical time (as given from plots such as Fig. 5), this trend is reversed. Fig. 7 shows that the critical time, defined according to vacancy concentration without consideration of error bars, decreases as radiation temperature increases.

To further understand how atomic processes affect the vacancy accumulation, we compare the number of vacancies annihilated at GBs and the number of vacancies annihilated by bulk recombination with interstitials. For two grain sizes of 25 nm and 40 nm, the radiation conditions are $P = 10^{-5}$ dpa/s, $T = 0.25T_m$. Fig. 8a shows that bulk recombination in grains of 40 nm is responsible for *more* vacancy annihilation than in grains of 25 nm; the difference without consideration of error bars is $\Delta 1$. Conversely, GB absorption is responsible for *fewer* annihilated vacancies in grains of 40 nm than in grains of 25 nm; the difference without consideration of error bars is $\Delta 2$. If GB absorption dominates, vacancy accumulation increases with grain size; otherwise, the opposite dependence is observed. The relative dominance of GB absorption and bulk recombination is shown as the difference $\Delta 2 - \Delta 1$ in Fig. 8b. During the transient stage (early stage of time), interstitials more quickly diffuse to GBs in smaller grains, leaving fewer interstitials to recombine with vacancies. As a result, the vacancy accumulation in smaller grains is larger. After the transient stage, more vacancies diffuse to GBs in smaller grains, resulting in smaller vacancy accumulation in smaller grains. The competition of vacancies absorption at GBs and their bulk recombination with interstitials, which also diffuse to GBs, leads to the transient dependence of vacancy accumulation on grain size.

Before closing, we discuss the reported anomaly in historical context – in terms of comparison with previous studies and generalization. In retrospect, previous studies have alluded to the existence of the reported anomaly. Lam [14] has reported a crossover in defect concentration at low temperatures as a function of *distance* from a sink; similar reports have been conjectured in other reports [15–17]. In contrast, the anomaly reported here involves defect concentration as a function of grain size. The report of Lam is based on the same mechanism as in this paper, although our work specifically examines the dependence on grain size. In terms of generalization, two aspects are worth mentioning. First, the reported anomaly is the result of competition between vacancy-interstitial bulk recombination and vacancy absorption at sinks. Even if the sinks are not grain boundaries (e.g., nanoparticle–matrix interfaces in large grains), a similar transient anomaly can also be expected. Second, the reported anomaly is associated with Frenkel pair production mimicking electron radiation in grain interior, and generalization to neutron radiation of nuclear materials requires further studies – including the effects of cascade production [4], defect production near grain boundaries, and presence of helium gas atoms [18].

4. Conclusion

Based on atomistic simulations, we report the discovery of a new transient anomaly in the dependence of defect accumulation on grain size under Frenkel pair production mimicking electron radiation. During the transient stage, because interstitials diffuse faster than vacancies, few interstitials are available for recombination with vacancies in the bulk. As a result, vacancy accumulation in smaller grains is larger than in larger grains. The duration of the transient phase is longer for larger grains than for smaller grains, and it decreases as radiation temperature increases. The transient anomaly is the result of two competing atomic processes: GB absorption and bulk recombination of radiation produced defects.

Acknowledgements

Authors gratefully acknowledge financial support from Defense Threat Reduction Agency (HDTRA1-09-1-0027) and National Science Foundation (CMMI-0625602 and DMR-0906349); and thank Stas Golubov, Roger Stoller, Sidney Yip and Dieter Wolf for discus-

sions on radiation damage, and Shree Krishna and Suvranu De for enlightening discussions on FEM analyses.

References

[1] R. Bullough, B.L. Eyre, K. Krishan, Proc. Roy. Soc. Lond. A 346 (1975) 81.
[2] L.K. Mansur, M.H. Yoo, J. Nucl. Mater. 85–86 (1979) 523.
[3] S.J. Zinkle, Phys. Plasmas 12 (2005) 058101.
[4] C.H. Woo, B.N. Singh, F.A. Garner, J. Nucl. Mater. 191–194 (1992) 1224.
[5] B.N. Singh, Philos. Mag. 29 (1974) 25.
[6] H.C. Huang, G.H. Gilmer, T. Diaz de la Rubia, J. Appl. Phys. 84 (1998) 3636.
[7] G.H. Gilmer, H.C. Huang, T. Diaz de la Rubia, J.D. Torre, F. Baumann, Thin Solid Films 365 (2000) 189.
[8] H.C. Huang, G.H. Gilmer, J. Comput.-Aided Mater. Des. 7 (2001) 203.
[9] H.C. Huang, L.G. Zhou, J. Comput.-Aided Mater. Des. 11 (2004) 59.
[10] R. Lennartz, F. Dworschak, H. Wollenberger, J. Phys. F 7 (1977) 2011.
[11] Y. Mishin, M.J. Mehl, D.A. Papaconstantopoulos, A.F. Voter, J.D. Kress, Phys. Rev. B 63 (2001) 224106.
[12] J.R. Hu, S.C. Chang, F.R. Chen, J.J. Kai, Scr. Mater. 45 (2001) 463.
[13] V. Yamakov, D. Wolf, M. Salazar, S.R. Phillpot, H. Gleiter, Acta Mater. 49 (2001) 2713.
[14] N.Q. Lam, J. Nucl. Mater. 56 (1975) 125.
[15] D.I.R. Norris, Philos. Mag. 23 (1971) 135.
[16] S.A. Manthorpe, S.N. Buckley, Proc. Brit. Nucl. Energy Soc. Eur. Conf. (1971) 239.
[17] R. Sizmann, J. Nucl. Mater. 69–70 (1978) 386.
[18] H.C. Huang, N. Ghoniem, J. Nucl. Mater. 212–215 (1994) 148.